Synthesis and Spontaneous Polymerization of Oligo(ethylene glycol)-Conjugated Benzofulvene Macromonomers. A Polymer Brush Forming a Physical Hydrogel

Andrea Cappelli,*,† Simone Galeazzi,† Germano Giuliani,† Maurizio Anzini,† Mario Grassi,‡ Romano Lapasin,‡ Gabriele Grassi,§ Rossella Farra,|| Barbara Dapas,|| Marianna Aggravi,⊥ Alessandro Donati,⊥ Lucia Zetta,# Antonella Caterina Boccia,# Fabio Bertini,# Filippo Samperi,▽ and Salvatore Vomero†

Dipartimento Farmaco Chimico Tecnologico and European Research Centre for Drug Discovery and Development, Università degli Studi di Siena, Via A. Moro, 53100 Siena, Italy, Department of Chemical Engineering DICAMP, University of Trieste, Piazzale Europa 1, I-34127, Trieste, Italy, Department of Life Sciences, University of Trieste, Via Giorgeri 7, I-34127, Trieste, Italy, Department of Clinical, Morphological and Technological Sciences, University Hospital of Cattinara, Strada di Fiume 447, I-34149, Trieste, Italy, Dipartimento di Scienze Chimiche e dei Biosistemi, Università degli Studi di Siena, Via A. Moro, 53100 Siena, Italy, Istituto per lo Studio delle Macromolecole (CNR), Via E. Bassini 15, 20133 Milano, Italy, and Istituto di Chimica e Tecnologia dei Polimeri (CNR), Viale A. Doria 6, 95125 Catania, Italy

Received October 30, 2008; Revised Manuscript Received February 2, 2009

ABSTRACT: Two methyl end-capped oligo(ethylene glycol) esters (**1a**,**b**) of benzofulvene derivative **BF1** were synthesized and induced to polymerize spontaneously by solvent removal to give poly-**1a**,**b** showing both NMR and absorption/emission spectra very similar to those of poly-**BF1**. Poly-**1a**,**b** showed relatively high molecular weight and the tendency to depolymerize to a different degree as a function of the temperature in the presence of solvents, while they exhibited appreciable stability in the absence of solvent. Poly-**1b**, bearing a longer oligo(ethylene glycol) side chain, featured an amphiphilic character and interacted with a number of organic solvents to produce transparent gel aggregates, and with water to give a quite compact physical gel. Rheological studies performed on the hydrogel suggested strong gel characteristics and the combination of rheology and NMR transverse relaxation measurements allowed the pore size distribution in the hydrogel to be defined. Finally, biological studies performed with poly-**1b** solutions showed neither cytotoxicity nor cell viability impairment suggesting potential biocompatibility features for this polymer. In conclusion, poly-**1b** can be considered a promising polymer for the preparation of hydrogels potentially useful in a range of biological and biotechnological applications such as drug delivery, molecular recognition, biosensing, protein and DNA separation, micro- and nanofluidics, as well as tissue engineering.

1. Introduction

Poly(ethylene glycol) (PEG) is one of the most frequently studied and used polymers in the pharmaceutical field because of its various valuable features. Indeed, PEG is an inexpensive, water-soluble, biocompatible, and FDA-approved polymer. In fact, PEG can confer solubility in the physiological environment and prevent the interaction with plasma proteins and cells, and is therefore used as shielding agent for in vivo delivery of several bioactive compounds.[1,2] Moreover, PEG is used to shield drug carriers such as liposomes and nanoparticles.[3,4]

A recent approach to the covalent conjugation of PEG (permanent PEGylation) with carrier polymeric matrices is represented by the polymerization of the preformed PEG macromonomers such as oligo(ethylene glycol) methacrylate (OEGMA).[5−11] In particular, Ishizone and co-workers used anionic polymerization of methacrylates showing short oligo(ethylene glycol) alkyl ether side chains to obtain poly[oligo(ethylene glycol) alkyl ether methacrylate]s characterized by different water solubility and lower critical solution temperature (LCST) depending on both the length and the terminal substituent of the hydrophilic OEG side chains.[9] On the other hand, atom transfer radical polymerization (ATRP) of a commercially available OEGMA derivative was performed in aqueous media under remarkably mild conditions to obtain OEGMA polymers showing low polydispersities.[10,11] Moreover, ATRP of 2-(2-methoxyethoxy)ethyl methacrylate with OEGMA gave poly(MEO_2MA-*co*-OEGMA) copolymers showing controlled chain length, narrow molecular weight distribution, interesting solution properties in water, and tunable thermosensivity.[6] Finally, homo- or copolymerization of macromonomers (the so-called "grafting through" method) has been used in the synthesis of cylindrical polymer brushes, which have received a great deal of attention in very recent times.[12]

We recently reported that the spontaneous polymerization of benzofulvene derivative **BF1** (Scheme 1) gave a new hydrophobic polymer (poly-**BF1**) showing vinyl structure stabilized by aromatic stacking interactions.[13,14] Poly-**BF1** obtained by spontaneous polymerization (poly-**BF1-SP**) shows very high molecular weight, high solubility in the most common organic solvents, a thermoreversible polymerization/depolymerization, and the tendency to give fractal-like macromolecular aggregates.[14]

* Corresponding author. Telephone: +39 0577 234320. Fax: +39 0577 234333. E-mail: cappelli@unisi.it.
† Dipartimento Farmaco Chimico Tecnologico and European Research Centre for Drug Discovery and Development, Università degli Studi di Siena.
‡ Department of Chemical Engineering DICAMP, University of Trieste.
§ Department of Life Sciences, University of Trieste.
|| Department of Clinical, Morphological and Technological Sciences, University Hospital of Cattinara.
⊥ Dipartimento di Scienze Chimiche e dei Biosistemi, Università degli Studi di Siena.
Istituto per lo Studio delle Macromolecole (CNR).
▽ Istituto di Chimica e Tecnologia dei Polimeri (CNR).

10.1021/ma802429g CCC: $40.75
Published on Web 03/09/2009

Scheme 1. Structure of Benzofulvene Derivatives

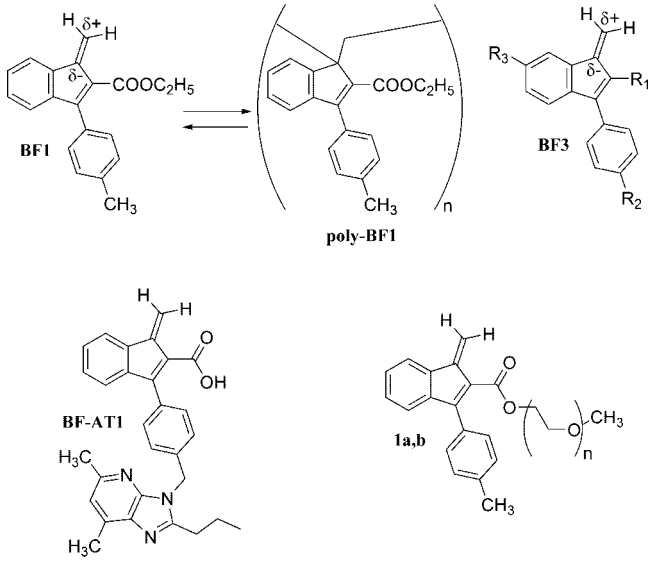

Conversely, the anionic polymerization of **BF1** produced a mixture of oligomers and a polymer (poly-**BF1-AP**), which is characterized by a significantly lower molecular weight with respect to that shown by poly-**BF1-SP** and the tendency to aggregate in nanospheres and microspheres.[15]

A polybenzofulvene derivative related to poly-**BF1** was shown to release the bioactive monomer (**BF1-AT1**, an angiotensin II AT_1 receptor antagonist) in the test conditions simulating the physiological environment.[16] Additionally, the synthesis of a series of benzofulvene derivatives **BF3** was described. These *trans*-diene derivatives showed spontaneous polymerization/depolymerization and the results obtained demonstrated that most of poly-**BF3** properties (e.g., formation, molecular weight, structure, thermoreversibility, and aggregation in nanostructured entities) may be modulated by the stereoelectronic characteristics of the substituents present on the indene moiety.[17]

These results, along with the similarities of **BF1** with methacrylates and cyanoacrylates, stimulated the synthesis of methyl end-capped oligo(ethylene glycol) conjugates of **BF1** (MOEG-**BF1**) in the form of esters **1a**,**b** in order to evaluate their tendency toward spontaneous polymerization and to find out the properties of the resulting polymers. The present paper reports on the synthesis of novel polybenzofulvene derivatives, in which oligomeric PEG side chains play a key role in determining intriguing features such as an amphiphilic character, which together with the polymer brush configuration is capable of inducing the formation of a physical and biocompatible hydrogel.

2. Results and Discussion

2.1. Synthesis of Poly-1a,b. The preparation of MOEG-conjugated benzofulvene macromonomers **1a**,**b** was carried out starting from indenones **2a**,**b** as reported in Scheme 2. The reaction of **2a**,**b** with trimethylaluminium afforded indenol derivatives **3a**,**b**, which were dehydrated in chloroform or $CDCl_3$ in the presence of *p*-toluenesulfonic acid (PTSA) to give *trans*-diene derivatives **1a**,**b**. The dehydration performed in $CDCl_3$, allowed the ^{1}H NMR analysis to be performed without the elimination of the solvent and clear ^{1}H NMR spectra compatible with the structures of **1a**,**b** were obtained. *trans*-Diene derivatives **1a**,**b** were relatively stable in solution and polymerized upon solvent removal to give poly-**1a,b**.

The required indenones **2a**,**b** were synthesized by reaction of acid **4**[17] with the appropriate monomethyl OEG chains **6a,b**

Scheme 2. Synthesis of MOEG-Conjugated Polybenzofulvene Derivatives Poly-1a,b[a]

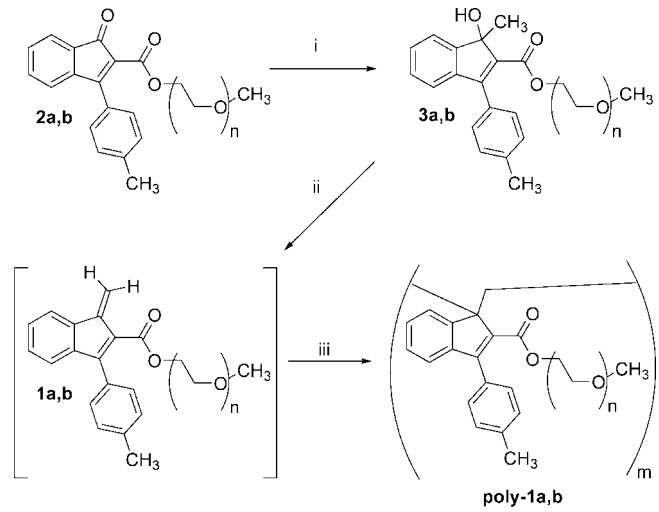

[a] Structures: **1a**, $n = 3$; **1b**, $n = 9$. Reagents: (i) $Al(CH_3)_3$, CH_2Cl_2; (ii) PTSA, $CHCl_3$; (iii) solvent elimination.

Scheme 3. Synthesis of Indenone Derivatives 2a,b[a]

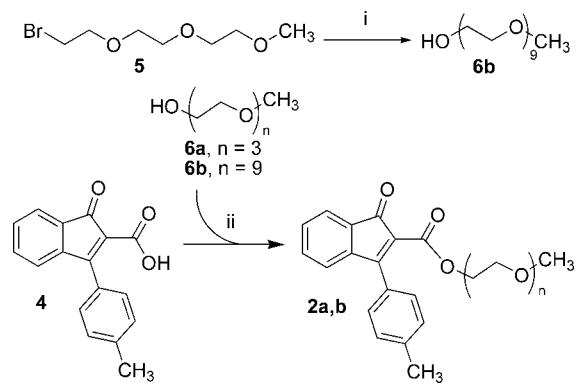

[a] Reagents: (i) $HO(CH_2CH_2O)_6H$, NaH, toluene; (ii) EDC, DMAP, CH_2Cl_2.>

in the presence of EDC and DMAP. While **6a** is a commercially available intermediate, compound **6b** was synthesized starting from bromide **5**[18] and hexa(ethylene glycol) as outlined in Scheme 3.

2.2. Properties of Poly-1a,b. Poly-**1a** was obtained as a pale yellow glassy solid, while poly-**1b** was a colorless elastic sticky one.

Freshly prepared poly-**1a** appeared to be soluble in chloroform, whereas an apparent decrease in the dissolution rate was observed after a prolonged storage as a glassy solid. Poly-**1b** was insoluble in nonpolar organic solvents such as cyclohexane, while interacting with polar organic solvents [e.g., chloroform, THF, DMF, *N*,*N*-dimethylacetamide (DMA), DMSO, ethanol, and methanol] and with water generating transparent gel aggregates. The gel swelling was quite fast in chloroform (the best among the above-cited solvents) and slower in DMSO, DMF, DMA, ethanol, and methanol so that the complete dissolution of the aggregates occurred after a time variable from few weeks to several months at room temperature. On the other hand, the hydrogel was proved to be more compact. The addition of water to the solutions of poly-**1b** in THF, DMA, or ethanol did not determine the precipitation of the polymer and the presence of poly-**1b** could be detected by absorption and emission spectroscopy. These results suggest that poly-**1b** is

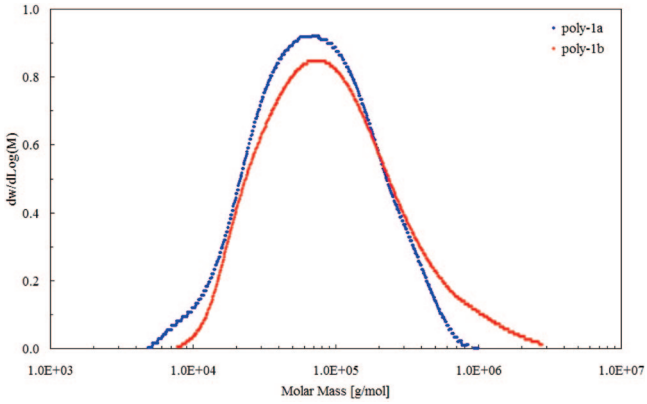

Figure 1. Differential MWD of poly-**1a** (blue) and poly-**1b** (red) samples.

capable of forming gels stabilized by weak noncovalent interactions (i.e., MOEG chain entanglement), which are weakened by solvation thus giving the macromolecule release into the bulk of the solvent.

When poly-**1b** was swollen in ethanol at room temperature for one week and the ethanol excess was removed from the gel aggregates and replaced with deuterium oxide, no evident changes were observed in the gel appearance. Moreover, after equilibration in deuterium oxide for several days at room temperature into a NMR tube, the gentle warming of the biphasic system at about 35 °C generated visible transformations in both the components. The solution became cloudy and the gel turned from transparent to white. ^{1}H NMR spectroscopy showed in the solution the presence of a relevant amount of ethanol along with a small amount of poly-**1b**. These results suggest that isolated macromolecules and ethanol molecules are capable of migrating from the initial organogel to the bulk water and they support thermoresponsive features for poly-**1b**.

In conclusion, the most intriguing property of these poly-MOEG-BF1 derivatives is the fact that the presence of relatively long MOEG chains as in poly-**1b** allows the interaction with water and the formation of a quite compact physical gel. Because of the important role played by hydrogels in several fields of the material and life sciences, the properties of poly-**1b** hydrogel were characterized in detail and the results of such studies are described in the relevant section (see below).

2.2.1. Molecular Weight Distribution Characterization. The molecular weight distribution (MWD) characterization of poly-**1a**,**b** was performed by means of a multiangle laser light scattering (MALS) detector online to a size exclusion chromatography (SEC) system using chloroform as the mobile phase. Poly-**1a**,**b** samples used in MWD studies were completely dissolved in chloroform without significant aggregation. The differential MWD of poly-**1a**,**b** samples obtained by the SEC-MALS system is shown in Figure 1. The weight-average molecular weight M_w of the two samples is relatively high (108 and 175 kg/mol for poly-**1a** and poly-**1b**, respectively) and the polydispersity index M_w/M_n, where M_n denotes the numeric-average molecular weight, is broader (2.4 and 3.0 for poly-**1a** and poly-**1b**, respectively) with respect to that measured for poly-BF1 (1.6−2.0).[14,15]

2.3. Structure of Poly-1a,b. *2.3.1. NMR.* In order to evaluate the influence of MOEG side chains on the poly-**1a**,**b** structure, the ^{13}C NMR spectra of the two polymers were compared with that of poly-**BF1** obtained by spontaneous polymerization (poly-**BF-SP**, Figure 2). This comparison suggests that spontaneous polymerization of **1a** occurs with the same mechanism of poly-**BF1-SP** formation. In fact, the aromatic regions of poly-**BF1-SP** and poly-**1a** spectra are practically indistinguishable and the peaks attributable to C-1 and C-D (the carbon atoms forming the polymer backbones) show similar chemical shift values in the ^{13}C spectra of both polymers. In other words, the presence of the short oligomeric PEG side chains of **1a** appears to have negligible effect on the structure of the polymer backbone. However, the spectrum of poly-**1a** shows a large difference in the line width of the signals due to the polybenzofulvene backbone compared to those due to the MOEG side chains. This selective line broadening can be easily explained with the different mobility that might characterize backbone and side chains of the polymer. In fact, this feature is even more evident in the spectrum of poly-**1b** (Figure 2), in which a possibly much lower mobility of the backbone, with respect to the MOEG side chains, makes the backbone carbon signals not so clear-cut even after prolonged acquisition times.

2.3.2. Absorption and Emission Spectroscopy. The UV−vis absorption spectra of poly-**1a**,**b** (Figure 3) almost perfectly match that of poly-**BF1-SP** and show the existence of two absorption components: one centered around 240−242 nm attributable to the 3-phenylindene moiety and a second centered at about 288 nm related to the presence of an extended π-conjugation (e.g., a cinnamate moiety can be recognized in the monomeric unit of the three polymers).

Similarly, the emission spectra of poly-**1a**,**b** (Figure 4) are identical to that of poly-**BF1-SP** in showing the presence of a single broad peak centered around 445 nm, while both the models of poly-**BF1** monomeric units show maximum emissions at about 380 nm.[14]

It is generally recognized that the fluorescence in solution of a polymer with aromatic side groups is composed of monomer and excimer emissions. A comparative study performed on the poly-**BF3** series allowed to attribute the emission around 350−380 nm to nonstacked monomeric units and the peaks at 440−470 nm to the stacked ones.[17] This hypothesis was supported by Londergan's work attributing the predominant emission at 448 nm of a structurally related polymer to the formation of an excimer resulting from chromophore stacking, and the secondary peak at 347 nm to the monomer emission on the basis of the observation that 3-phenylindene (the model of the monomeric unit) shows an emission peak at 345 nm.[19]

In conclusion, the comparison of the absorption and emission spectra of poly-**BF1** obtained by spontaneous polymerization (poly-**BF1-SP**) with those of poly-**1a**,**b** suggests a similar degree of the π-stacking interactions among the aromatic moieties.

2.3.3. MALDI-TOF Mass Spectrometry. The structure and composition of the poly-**1a**,**b** was also confirmed by matrix-assisted laser desorption time-of-flight mass spectrometry (MALDI-TOF MS). The MALDI spectrum of poly-**1a**, (Figure 5) obtained with 2-(4-hydroxylphenylazo)benzoic acid (HABA) as a matrix, shows the presence of a series of peaks from 600 to 5000 Da, the interval between two principal peaks being 408.5 ± 0.2 Da, corresponding to the molecular mass of the poly-**1a** monomeric unit bearing the tri(ethylene glycol) monomethyl ether side chain ($n = 3$ in Scheme 2). In the case of poly-**1b**, the interval between two principal peaks was 672.6 ± 0.2 Da (Figure 5), which corresponds to the molecular mass of poly-**1b** monomeric unit having the nona(ethylene glycol) monomethyl ether side chain ($n = 9$ in Scheme 2), in agreement with the synthetic procedure. The most intense peaks in Figure 5 correspond to the sodiated-molecular ions of poly-**1a**,**b** oligomers. The macromolecular chains with a molecular mass higher than 5000 Da were undetectable under MALDI-TOF conditions, both polymers having a broad molar mass distribution (see Figure 1).[20,21] The mass spectrum of poly-**1b** sample shows also the presence of the peak at m/z 695.5 due to the sodiated ions of monomer **1b** (Scheme 2). These results confirm that the

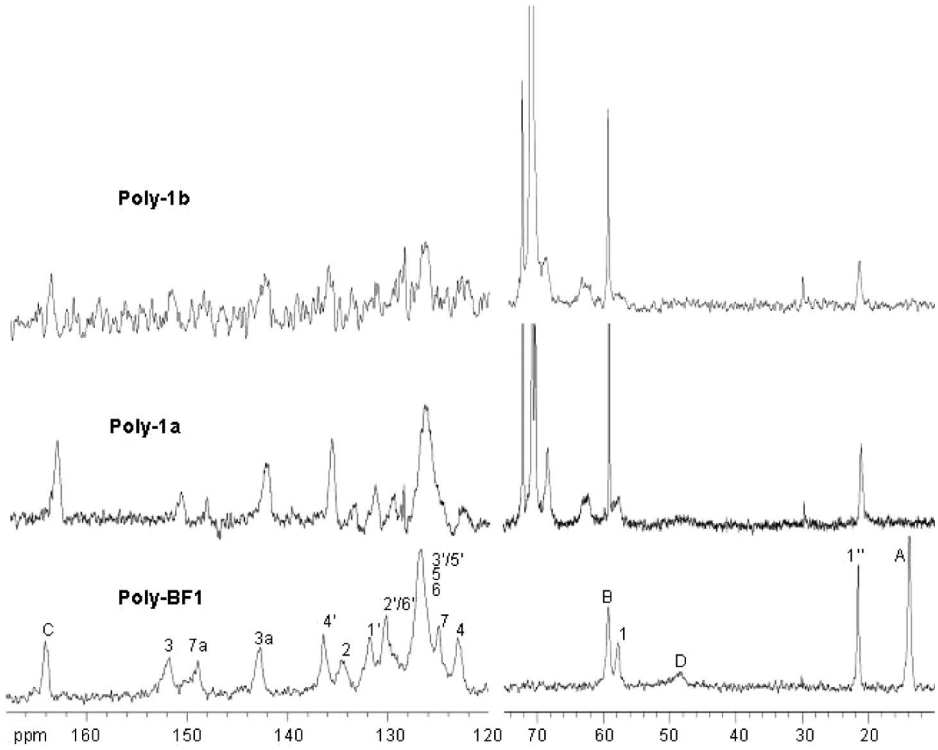

Figure 2. Comparison of the ^{13}C NMR ($CDCl_3$) spectra of poly-**1a**,**b** and poly-**BF1-SP**.

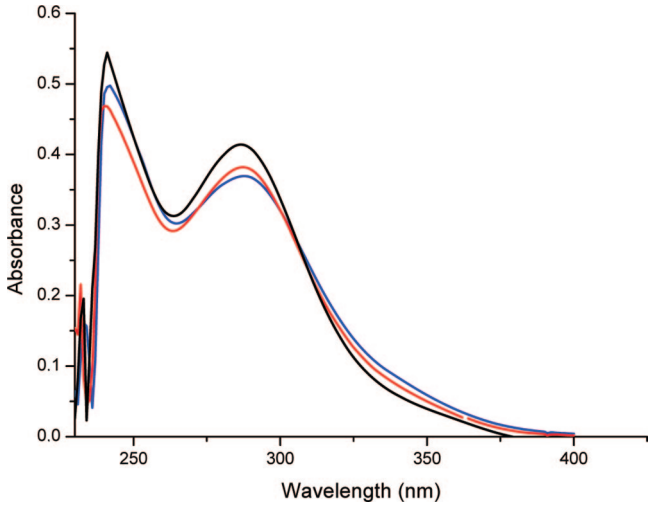

Figure 3. Comparison of the absorption spectra of poly-**1a** (red), poly-**1b** (blue), and poly-**BF1-SP** (black). The spectra were obtained in chloroform at room temperature. The concentration in monomer base unit was ca. 4.0×10^{-5} mol/L for all the polymers.

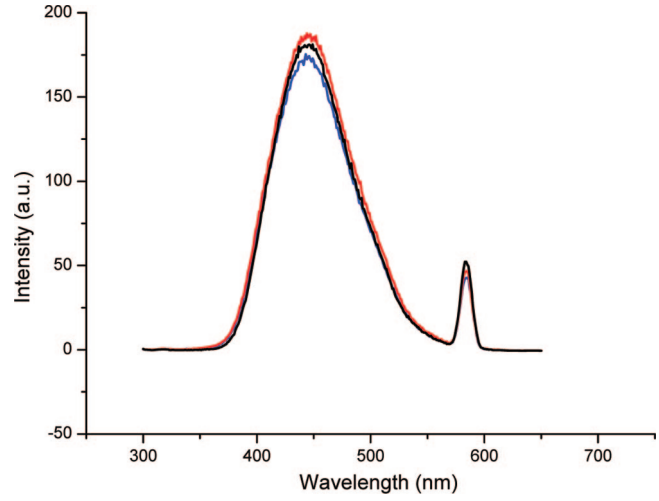

Figure 4. Comparison of the emission spectra of poly-**1a** (red), poly-**1b** (blue), and poly-**BF1-SP** (black). The spectra were obtained in chloroform at room temperature. The excitation wavelength was 288 nm for all the polymers. The peak at ca. 580 nm is the secondary scattering of the excitation beam.

spontaneous polymerization reaction occurs without breaking off the oligo(ethylene glycol) side chains.

2.4. Depolymerization Studies. Previous work[13,15] demonstrates that poly-**BF1** depolymerizes in different solvents and at different temperatures showing a behavior (unzipping) similar to that of cyanoacrylates.[22,23] Furthermore, poly-**BF1-AT1** was demonstrated to release the bioactive monomer (**BF1-AT1**) in the binding study conditions,[16] suggesting its potential degradability in the physiological environment. Therefore, thermoinduced depolymerization of poly-**1a**,**b** was studied in solution by ^1H NMR spectroscopy. Solutions of 5.0 mg of poly-**1a**,**b** in 0.5 mL of DMSO-d_6 were heated at 150 °C and ^1H NMR spectra were recorded at regular time intervals. Figure 6 suggests for poly-**1a**,**b** a thermoinduced depolymerization behavior similar to that shown by poly-**BF1** obtained by spontaneous polymerization.[17] In fact, an almost complete depolymerization was observed for the polymers after 3−6 h heating at 150 °C. Thus, further experiments were performed with poly-**1a**,**b** in order to evaluate a potential reversibility at a temperature close to the physiological one. ^1H NMR experiments performed with poly-**1a**,**b** in chloroform show that depolymerization is detectable after 2−3 weeks at room temperature and this result suggests promising biological applications of these polymers based on their degradation features.

2.5. Differential Scanning Calorimetry and Thermogravimetric Analysis. The thermal behavior of poly-**1b** in the absence of solvents was investigated by differential

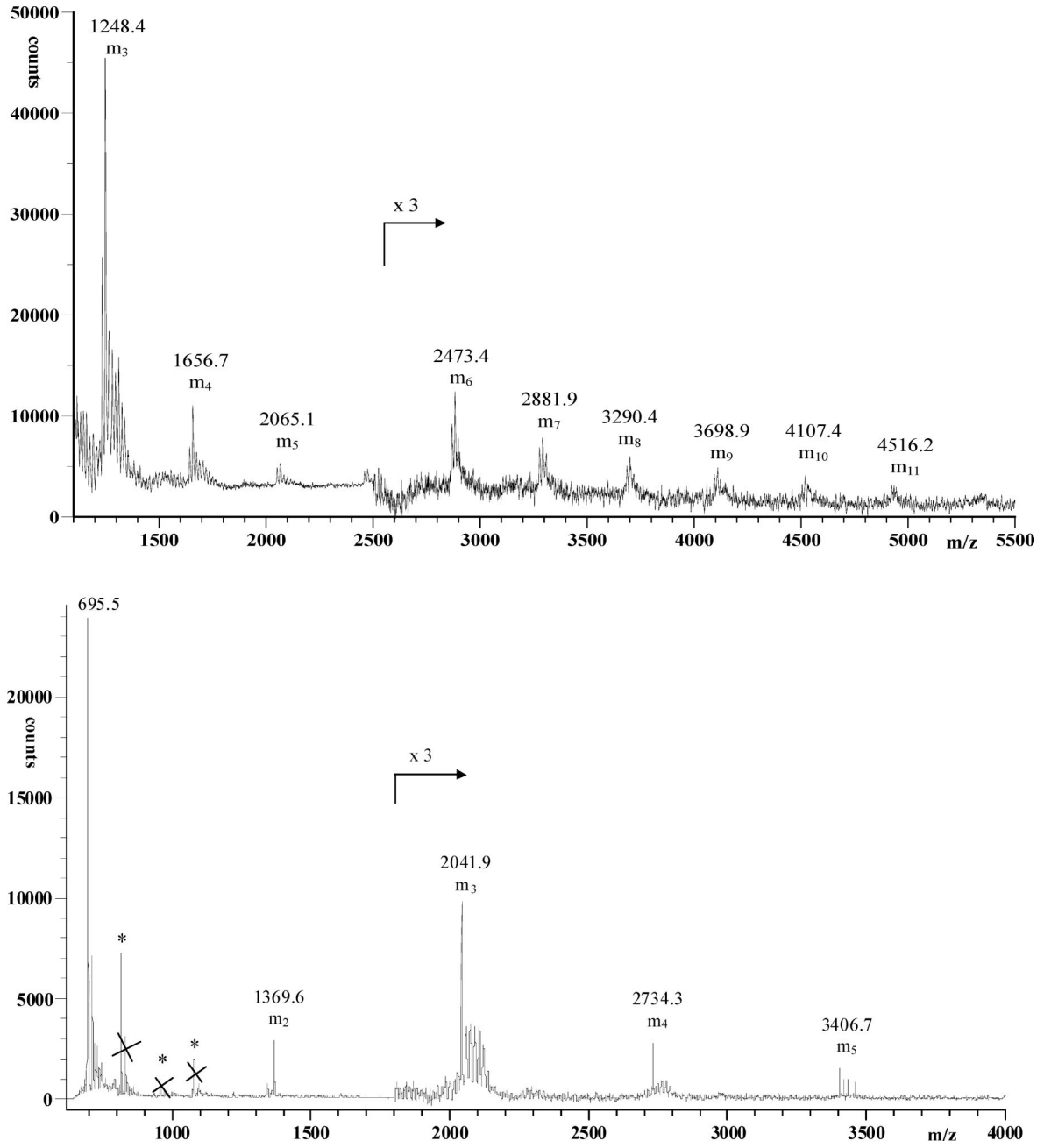

Figure 5. MALDI-TOF mass spectra of poly-**1a** (top) and poly-**1b** (bottom). Asterisks indicate clusters of matrix.

scanning calorimetry (DSC) and by thermogravimetric analysis (TGA). DSC analysis performed over a temperature range of 50−280 °C at a heating rate of 20 °C/min showed an endothermic peak centered at 215 °C with a heat flow of 85 J/g (Figure 7) significantly broader than that of poly-**BF1-SP**.[17]

Moreover, TGA showed that poly-**1b** (in solvent absence) is not subject to thermal degradation up to approximately 210 °C. In fact, poly-**1b** shows an initial small weight loss at about 215 °C and a quite sharp maximum of the derivative at 375 °C (Figure 8). If the broad endothermic peak at 215 °C in the DSC curve is assumed to represent depolymerization, the high value of DTG peak can be explained in terms of MOEG chain entanglement, which may hamper the monomer release, thus leading to weight loss.

2.6. Structural Properties of Poly-1b Hydrogel. The hydrogel was prepared by letting the dry polymer swell in distilled water at 25 °C up to system transparency (about 10 h). Then, the hydrogel was recovered from water and put into the measuring device (rheometer or low field NMR cell). In order to obtain information about macroscopic and microscopic structural characteristics, stress sweep (*SS*) and frequency sweep (*FS*) tests were performed at 25 °C. *SS* test revealed that the linear viscoelastic conditions were attained for deformation $\gamma < 0.9\%$. Accordingly, *FS* tests were executed at constant deformation $\gamma = 0.01\%$.

Figure 9 shows that the trends of the elastic (G') and viscous (G'') moduli versus pulsation ω ($=2\pi f$, f = solicitation frequency) are parallel. In addition, as G'' is always clearly higher than G'' (approximately 1 order of magnitude), we can state that the elastic properties are always predominant, this being typical of strong gels. Figure 9 also shows that G' and G'' trends can be satisfactorily fitted ($F(6,16,0.99) < 509$) by means of five Maxwell elements (mechanical devices each composed of a spring and a dashpot in series) placed in parallel whose relaxation times λ_i are scaled in factors of 10 (see solid lines).[24] Assuming that hydrogel shear modulus G is the sum

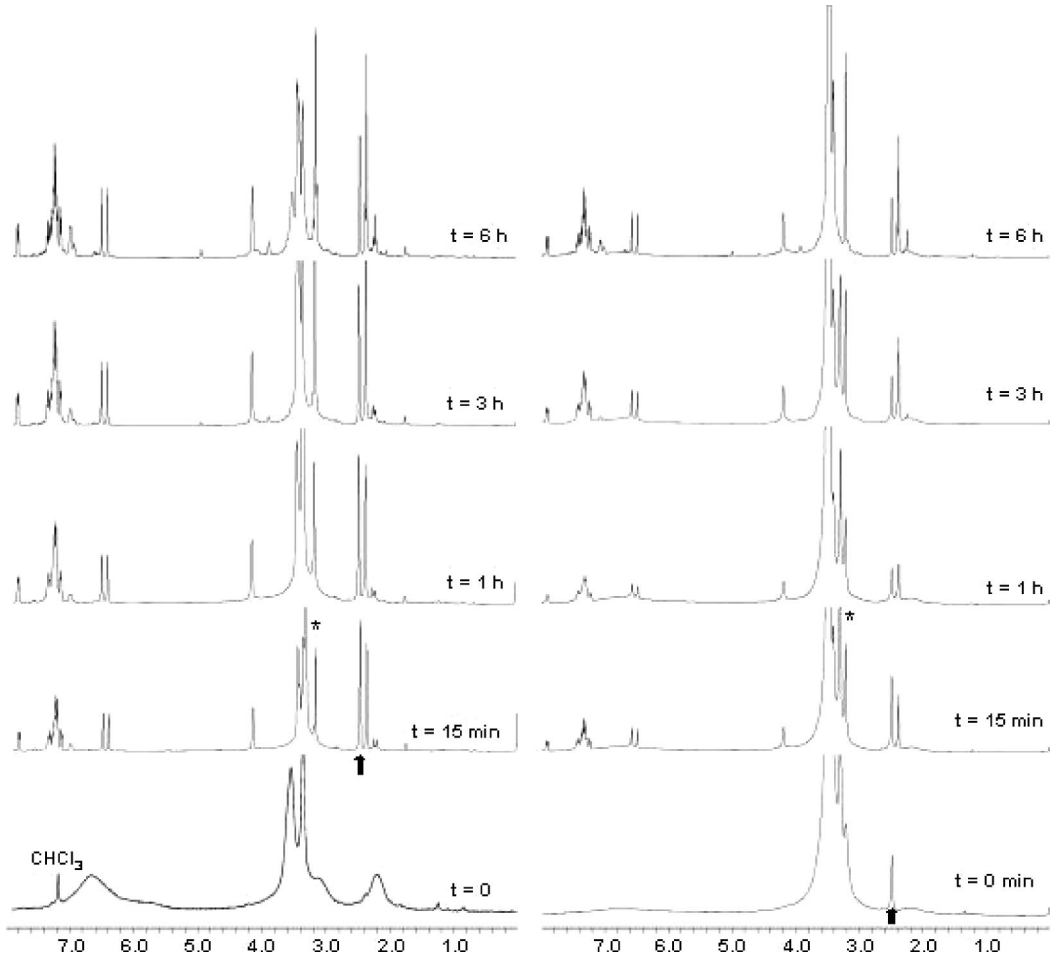

Figure 6. Thermoinduced depolymerization of poly-**1a** (left) and poly-**1b** (right) followed by ^{1}H NMR (400 MHz). Solutions of 5.0 mg of poly-**1a**,**b** in 0.5 mL of DMSO-d_6 were heated at 150 °C and ^{1}H NMR spectra were recorded at regular time intervals. The arrows indicate the DMSO peaks and the asterisks the water peak. Because of the low solubility of poly-**1a** in DMSO-d_6 at room temperature, the starting spectrum ($t = 0$) was performed in $CDCl_3$.

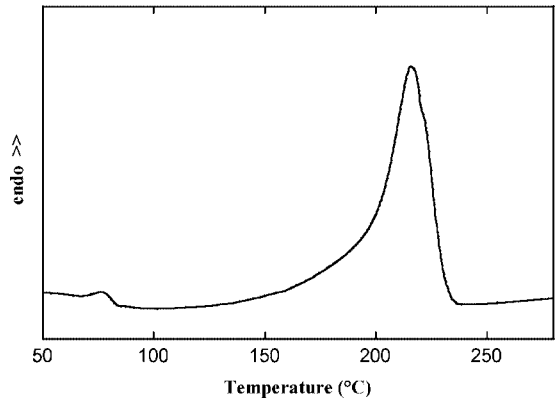

Figure 7. DSC curve of poly-**1b**.

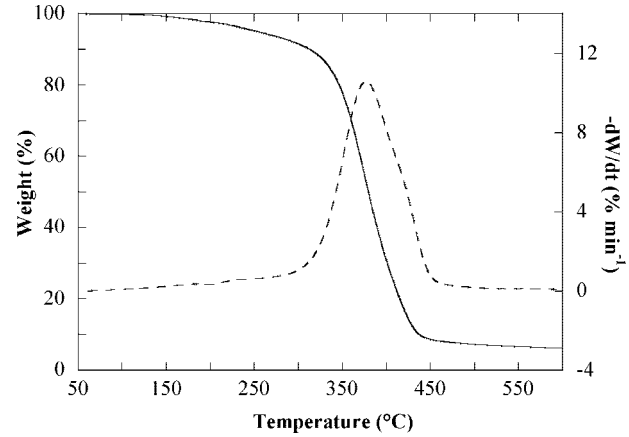

Figure 8. TGA (solid line) and DTG (dashed line) curves of poly-**1b.**

of the elastic contributes (G_i) of each Maxwell element,[25] hydrogel cross-link density ρ_x can be evaluated according to Flory's theory:[26]

$$\rho_x = \frac{G\nu_p^{2/3}}{RT} \quad (1)$$

where R is the universal gas constant, T is absolute temperature and ν_p is the polymer volume fraction in the gel. In our case, equation 1 yields $\rho_x = (6.6 \pm 1) \times 10^{-5}$ mol/cm^3 being $\nu_p = (0.13 \pm 0.01)$ and $G = (645000 \pm 21000)$ Pa. Interestingly, on the basis of the knowledge of ρ_x and the "equivalent network theory",[27] it is possible to estimate the average mesh size of the polymeric network. This theory replaces the polymeric network by an idealized network made of a collection of blobs whose diameter coincides with the average network mesh size φ according to the following relation:

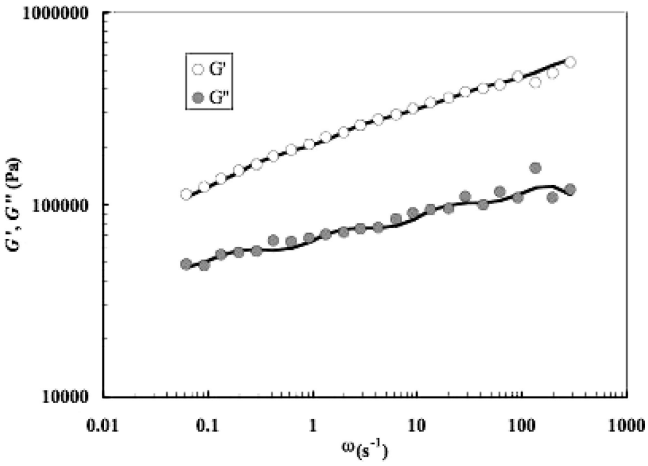

Figure 9. Hydrogel mechanical spectrum. Comparison between experimental elastic (G'; open circles) and viscous (G'', closed circles) moduli with five element Maxwell model best fitting (solid lines). ω is pulsation ($=2\pi f$, $f =$ solicitation frequency).

$$\varphi = \sqrt[3]{\frac{6}{\pi N_{av} \rho_x}} \tag{2}$$

where N_{av} is the Avogadro number. According to equation 2 we obtain $\varphi = (3.6 \pm 0.2)$ nm.

In order to obtain further information about hydrogel structure, a low field NMR characterization was undertaken, as this technique can provide useful information via the determination of the hydrogen atoms status.

Figure 10 showing hydrogel T_2 distribution evidence the existence of four peaks witnessing the existence of four conditions for the hydrogen atoms in the hydrogel. Remembering that we are not dealing with a perfectly homogeneous system (it is a sort of highly concentrated suspension of homogeneous gel particles), the existence of the four peaks can be explained as follows. On the basis of high transverse relaxation time ($T_{21} = 2252 \pm 2$ ms, $A_1 = 0.55$), the first peak on the right represents the amount of hydrogen atoms belonging to water, that is out of the ensemble of gel particles. Indeed, the presence of gel causes only a minor reduction on transverse relaxation (pure water hydrogen atoms transverse relaxation time at 25 °C is around 2500 ms). The second peak on the right ($T_{22} = 914 \pm 10$ ms, $A_2 = 0.18$) should correspond to hydrogen atoms belonging to the water entrapped among the gel particles. On the contrary, the third peak ($T_{23} = 261 \pm 2$ ms, $A_3 = 0.23$) should correspond to hydrogen atoms belonging to the water inside the gel particles. Finally, the fourth peak ($T_{24} = 43 \pm 4$ ms, $A_4 = 0.04$), because of low transverse relaxation time, should correspond to the polymer's hydrogen atoms. Two experimental results support the above interpretation. The first one concerns the effect of temperature on T_2 distribution. For this purpose, Figure 11 reports the area of each peak (A_i) versus the transverse relaxation time T_2 occurring in correspondence of peak maximum for three different temperatures (15, 25, and 30 °C).

It is evident that the peaks' areas are almost constant with temperature, whatever the transverse relaxation time (T_{2i}), T_{21} and T_{22} increase with temperature while T_{23} and T_{24} are almost constant. This indicates that peaks 1 and 2 represent water that is not strongly bound to a solid substrate as the effect of thermal energy (transverse relaxation time increases with temperature) is clearly visible. On the contrary, the temperature increase has a negligible effect on the transverse relaxation time corresponding to the third and fourth peaks (T_{23}, T_{24}). Thus, these peaks correspond to highly structured hydrogen atoms as it occurs to

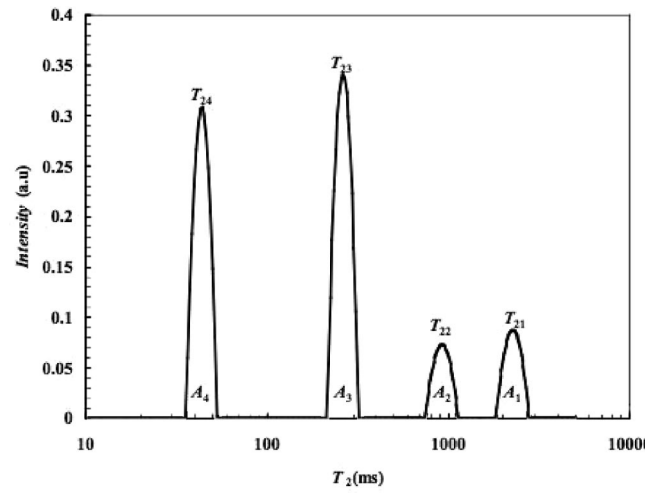

Figure 10. Hydrogel T_2 distribution. Four peaks (1, 2, 3 and 4) characterize hydrogel T_2 distribution. A_1, A_2, A_3, and A_4 indicate peak area while T_{21}, T_{22}, T_{23}, and T_{24} indicate the respective transverse relaxation time occurring at peak maximum.

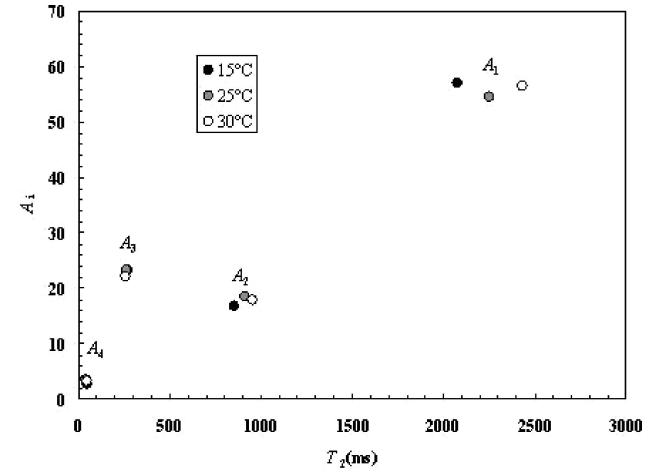

Figure 11. Temperature effect on T_2 distribution. Temperature increase produces the forward shifting of the transverse relaxation time T_2 corresponding to peaks 1 and 2 maximums. On the contrary, temperature has no significant effect on the position of peaks 3 and 4.

the hydrogen atoms belonging to water confined in or belonging to the polymeric network. The second experimental evidence supporting our interpretation of the T_2 distribution concerns hydrogel swelling ratio S_w defined as the ratio between hydrogel water (m_{H_2O}) and polymeric monomer m_m massive content. Indeed, remembering that the peak area is proportional to the number of hydrogen atoms relaxing with an average transverse relaxation time corresponding to peak maximum, S_w can be expressed by:

$$S_w = \frac{m_{H_2O}}{m_m} = \frac{N_m M_S}{N_{H_2O} M_m} \frac{A_3}{A_4} \tag{3}$$

where $N_{H_2O}(= 2)$ and N_m $(= 52)$ are, respectively, the number of hydrogen atoms in the water molecule and in the monomeric unit; $M_{H_2O}(= 18)$ and $M_m(= 673)$ are, respectively, water and monomer molecular weight, while A_4 and A_3 are, respectively, peak 4 (polymer) and 3 (water contained inside polymeric network) area. Interestingly, the S_w value according to eq. 3 (4.6) is not far from the experimental one (4.2) determined by measuring ($T = 25$ °C) the dry polymer weight increment at swelling equilibrium due to water absorption. Accordingly, it

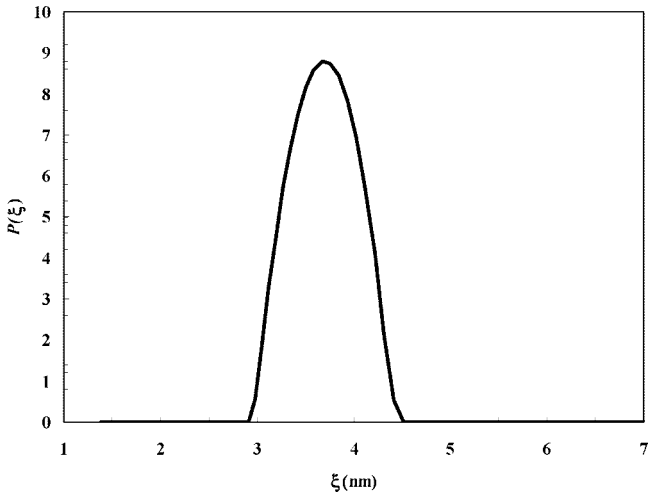

Figure 12. Hydrogel mesh size distribution. On the basis of information coming from mechanical and low field NMR spectra, it is possible to get the mesh size distribution expressed as the probability (P) of pore diameter ξ occurrence in the network.

is now possible to investigate further the hydrogel network structure remembering that the shape of peak 3 is closely correlated with the nanopore size distribution.[28] Indeed, as it is well-known[29] that the T_2 of nanopore water hydrogen atoms is proportional to nanopore diameter ξ via a constant (k) depending only on pore geometry (spherical, cylindrical, and so on) and inner surface properties, the information coming from rheology and low field NMR can be profitably combined to yield the nanopore size distribution. The evaluation of k is based on the relation existing between peak 3 average transverse relaxation time $\bar{T}_{23}$ and diameter φ:

$$\bar{T}_{23} = \frac{\int_{T_{23\min}}^{T_{23\max}} I_3(T_2)*T_2*\,\mathrm{d}T_2}{\int_{T_{23\min}}^{T_{23\max}} I_3(T_2)\,\mathrm{d}T_2} \overset{T_2=k\xi}{=} \frac{k^2\int_{k_2\xi_{23\min}}^{k_2\xi_{23\max}} I_3(\xi)*\xi\,*\mathrm{d}\xi}{k\int_{k_2\xi_{23\min}}^{k_2\xi_{23\max}} I_3(\xi)*\,\mathrm{d}\xi} = k\varphi \overset{\text{eq 2}}{=} k\sqrt[3]{\frac{6}{\pi N_{\mathrm{av}}\rho_x}} \quad (4)$$

where $I_3(T_2)$ is peak 3 local intensity, $T_{23\max}$ (or $\xi_{23\max}$) and $T_{23\min}$ (or $\xi_{23\min}$) indicates peak 3 extension in terms of transverse relaxation time (or pore diameter). Thus, k can be evaluated as:

$$k = \bar{T}_{23}\Big/\sqrt[3]{\frac{6}{\pi N_{\mathrm{av}}\rho_x}} = 71.2(\mathrm{ms/nm}) \quad (5)$$

Once T_2 is converted into length, peak 3 shape (see Figure 10) allows to calculate the probability P that each pore diameter has to be found in the polymeric network. Indeed, P is equal to the ratio between peak 3 area relating to the specific diameter and whole peak 3 area. The resulting P distribution is shown in Figure 12.

In the light of this mesh size, poly-**1b** hydrogel could efficiently act as a controlled delivery system for small molecules, characterized by van der Waals radii (r_{vdW}) lower than 1.25 nm such as theophylline (0.37 nm) and vitamin B12 (0.85 nm).[30] Interestingly, on the basis of the Peppas and Lustig theory,[31] we can roughly evaluate the reduction of theophylline and vitamin B12 diffusion coefficients in our gel system according to:

$$D_{\mathrm{g}}/D_{\mathrm{w}} \approx \left(1 - \frac{2r}{\phi}\right)\mathrm{e}^{-[\nu_{\mathrm{p}}/(1-\nu_{\mathrm{p}})]} \quad (6)$$

where D_{g} and D_{w} are the drug diffusion coefficient in the gel and in water, respectively, r is the drug's van der Waals radius while ν_{p} is polymer volume fraction in the swollen state ($\nu_{\mathrm{p}} = 0.13$ in our case). Equation 6 predicts $D_{\mathrm{g}}/D_{\mathrm{w}} = 0.68$ and 0.45 for theophylline and vitamin B12, respectively.

2.7. Biological Properties of Poly-1b. In order to evaluate its biological impact, poly-**1b** was mixed with water at 42 °C for 30 h under vigorous shaking to allow the dissolution of the greater part of the polymer. Poly-**1b** solution was tested in the hepatocellular carcinoma cells HepG2 and JHH6 displaying a different phenotype, hepatocyte-like for HepG2 and undifferentiated for JHH6.[32] Up to a polymer concentration of 50 μM (in monomer base unit, as determined by UV detection at 290 nm) and after two days of incubation, neither cytotoxicity induction nor cell viability impairment, as evaluated by LDH and MTT tests, respectively (Figure 13), were observed. The fact that not only the more resistant and undifferentiated JHH6 but also the differentiated HepG2 cells did not show any relevant negative effects, allows to assume a negligible impact of the polymer considered on the cell biology under our experimental conditions.

3. Conclusions

Two oligo(ethylene glycol) methyl ether conjugates of **BF1** (MOEG-**BF1**) were synthesized in order to evaluate their propensity toward spontaneous polymerization and to investigate the properties of the resulting polymers. MOEG-**BF1** derivatives **1a**,**b** appeared to polymerize by solvent removal (in the apparent absence of catalysts) with the same modalities shown by **BF1**. Indeed, poly-**1a**,**b** showed NMR features and absorption/emission spectra very similar to those shown by poly-**BF1-SP**. Moreover, MWD studies showed for poly-**1a**,**b** a relatively high molecular weight and moderately broad polydispersity indexes. In depolymerization experiments performed in the presence of solvents, poly-**1a**,**b** showed a behavior similar to that shown by poly-**BF1** with the peculiarity that low monomer concentrations were detected in $CDCl_3$ at room temperature after 2−3 weeks. This result suggests that poly-**1a**,**b** depolymerization is slow, but detectable at room temperature.

Poly-(MOEG-**BF1**) bearing a longer MOEG side chain (poly-**1b**) shows an amphiphilic character and interacts with a number of organic solvent to originate transparent gel aggregates and with water to give a quite compact physical gel. The structural properties of the hydrogel were investigated by rheological studies, which suggested that elastic properties are always predominant, as it occurs in strong gels. On the other hand, the combination of rheology and NMR transverse relaxation measurements allowed the characterization of pore size distribution in the hydrogel. In the light of its small mean pore size, poly-**1b** hydrogel appears to be a matrix system in which small molecules can migrate at different rates, while larger molecular systems (e.g., large proteins, enzymes, metal and metal oxide nanoparticles, dendrimers and dendrimer-based assemblies, etc.) can be entrapped. Finally, biological studies performed on solubilized poly-**1b** showed neither cytotoxicity nor cell viability impairment suggesting potential biocompatibility for this polymer. In conclusion, poly-**1b** can be considered a promising polymer for the preparation of hydrogels potentially useful in a range of biological and biotechnological applications such as drug delivery, molecular recognition, biosensing, protein and DNA separation, micro- and nanofluidics, and tissue engineering.

4. Experimental Section

Synthesis. Melting points were determined in open capillaries in a Gallenkamp apparatus and are uncorrected. UV/vis spectra were recorded with a Shimadzu 260 spectrophotometer and the emission

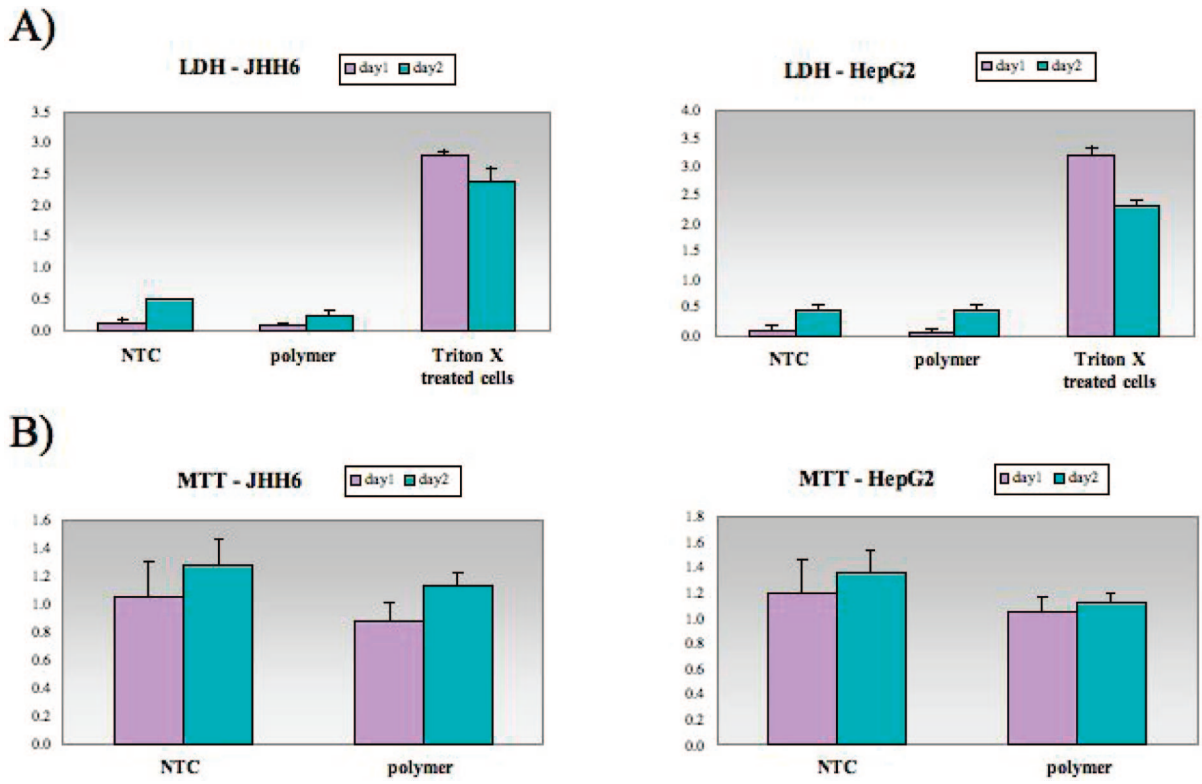

Figure 13. Polymer impact on cell biology. Citotoxicity (A) and cell viability (B) were evaluated by LDH and MTT tests, respectively, in human hepatocellular carcinoma cells JHH6 and HepG2 incubated at 37 °C in the presence of the solubilized polymer (50 μM) for one or two days; as a positive control for LDH test, triton X-100-treated cells (1% final concentration) were included. Data are shown as mean ± SD, $n = 3$. NTC = nontreated cells.

spectra were performed by means of a Shimadzu RF-5001PC instrument. Merck silica gel 60 (230−400 mesh) was used for column chromatography. Merck TLC plates, silica gel 60 F254 were used for TLC. ^{1}H NMR spectra were recorded at 200 MHz (Bruker AC200 spectrometer), at 400 MHz (Bruker DRX-400 AVANCE spectrometer), or 500 MHz (Bruker DRX-500 AVANCE spectrometer) in the indicated solvents (TMS as internal standard): the values of the chemical shifts are expressed in ppm and the coupling constants (*J*) in Hz. An Agilent 1100 LC/MSD operating with a electrospray source was used in mass spectrometry experiments. Microanalyses were carried out by means of a Perkin-Elmer Series II CHNS/O Analyzer 2400.

2,5,8,11,14,17,20,23,26-Nonaoxaoctacosan-28-ol (6b).[33] NaH (0.39 g, 16 mmol) was added to a solution of hexa(ethylene glycol) (5.5 mL, 22 mmol) in dry toluene (20 mL) and the resulting mixture was stirred at room temperature for 2 h. Then bromide **5**[18] (2.5 g, 11 mmol) was added and the reaction mixture was stirred at room temperature for one additional hour. The reaction mixture was then filtered, concentrated under reduced pressure and the residue was purified by flash chromatography with dimethoxyethane-*n*-exane (7:3) as the eluent to give **6b** as a colorless oil (2.4 g, yield 51%). ^{1}H NMR (200 MHz, $CDCl_3$): 2.85 (br s, 1H), 3.23 (s, 3H), 3.31−3.50 (m, 36H). MS (ESI): *m*/*z* 451 ($M+Na^+$).

2-[2-(2-Methoxyethoxy)ethoxy]ethyl 3-(4-Methylphenyl)-1-oxo-1*H*-indene-2-carboxylate (2a). A mixture of acid **4**[17] (2.0 g, 7.6 mmol) in dry dichloromethane (20 mL) with tri(ethylene glycol) monomethyl ether (**6a**) (1.2 mL, 7.6 mmol), EDC hydrochloride (1.7 g, 8.9 mmol), and DMAP (0.092 g, 0.76 mmol) was stirred overnight at room temperature. The reaction mixture was then concentrated under reduced pressure and the residue was purified by flash chromatography with dimethoxyethane-petroleum ether (3:7) as the eluent to yield indenone **2a**, as a yellow oil (2.1 g, yield 67%). ^{1}H NMR (200 MHz, $CDCl_3$): 2.38 (s, 3H), 3.29 (s, 3H), 3.52 (m, 10H), 4.26 (t, $J = 4.9$, 2H), 7.18 (m, 1H), 7.21−7.42 (m, 6H), 7.51 (m, 1H). MS(ESI): *m*/*z* 433 ($M + Na^+$).

2,5,8,11,14,17,20,23,26-Nonaoxaoctacosan-28-yl 3-(4-Methylphenyl)-1-oxo-1*H*-indene-2-carboxylate (2b). A mixture of acid **4**[17] (2.0 g, 7.6 mmol) in dry dichloromethane (20 mL) with nona(ethylene glycol) monomethyl ether (**6b**) (3.2 g, 7.5 mmol), EDC hydrochloride (1.7 g, 8.9 mmol), and DMAP (0.092 g, 0.76 mmol) was stirred overnight at room temperature. The reaction mixture was then concentrated under reduced pressure and the residue was purified by flash chromatography with dimethoxyethane-petroleum ether (6:4) as the eluent to yield indenone **2b**, as a yellow oil (3.5 g, yield 68%). ^{1}H NMR (200 MHz, $CDCl_3$): 2.40 (s, 3H), 3.33 (s, 3H), 3.48−3.69 (m, 34H), 4.27 (t, $J = 4.9$, 2H), 7.19 (m, 1H), 7.27 (m, 2H), 7.35−7.44 (m, 4H), 7.55 (m, 1H). MS(ESI): *m*/*z* 697 ($M + Na^+$).

General Procedure for the Synthesis of Indenol Derivatives 3a,b. To a solution of the appropriate indenone (**2a**,**b**) in dichloromethane (10 mL/1 mmol of indenone) was added a solution (2 M in THF) of $Al(CH_3)_3$, (2.5 equivalents) and the resulting mixture was stirred under nitrogen for 30 min. The $Al(CH_3)_3$ excess was cautiously decomposed with a 30% NaOH solution until the gas evolution ceased. The mixture was filtered and the filtrate was dried over sodium sulfate and evaporated under reduced pressure. Purification of the residue by flash chromatography with the appropriate eluent gave the corresponding indenol (**3a**,**b**).

2-[2-(2-Methoxyethoxy)ethoxy]ethyl 1-Hydroxy-1-methyl-3-(4-methylphenyl)-1*H*-indene-2-carboxylate (3a). This compound was obtained from indenone **2a** (0.84 g, 2.05 mmol) and purified by flash chromatography with dimethoxyethane-petroleum ether (3:7) as the eluent to give **3a** as a colorless oil (0.72 g, yield 82%). ^{1}H NMR (200 MHz, $CDCl_3$): 1.76 (s, 3H), 2.38 (s, 3H), 3.29 (s, 3H), 3.50 (m, 10H), 3.76 (br s, 1H), 4.22 (t, $J = 4.8$, 2H), 7.12−7.37 (m, 7H), 7.52 (m, 1H). MS(ESI): *m*/*z* 449 ($M + Na^+$).

2,5,8,11,14,17,20,23,26-Nonaoxaoctacosan-28-yl 1-Hydroxy-1-methyl-3-(4-methylphenyl)-1*H*-indene-2-carboxylate (3b). This compound was obtained from indenone **2b** (3.5 g, 5.2 mmol) and purified by flash chromatography with dimethoxyethane-petroleum

ether (6:4) as the eluent to give **3b** as a colorless oil (2.6 g, yield 72%). ^{1}H NMR (200 MHz, $CDCl_3$): 1.73 (s, 3H), 2.36 (s, 3H), 3.31 (s, 3H), 3.41−3.59 (m, 34H), 4.21 (t, J = 4.6, 2H), 7.11 (m, 1H), 7.18−7.37 (m, 6H), 7.51 (m, 1H). MS(ESI): m/z 713 (M + Na^+).

General Procedure for the Preparation of Solutions of Benzofulvene Macromonomers 1a,b in Chloroform or $CDCl_3$. A mixture of the appropriate indenol derivative (**3a**,**b**) in chloroform or $CDCl_3$ (10 mL/1 mmol of indenol) with a catalytic amount of *p*-toluenesulfonic acid monohydrate (PTSA) (0.2 equivalents) was heated under reflux for the appropriate time (typically from 2 to 4 h) and cooled to room temperature. The reaction mixture was washed with a saturated solution of $NaHCO_3$ and dried over sodium sulfate to afford a stock (about 0.1 M) solution of the corresponding monomer (**3a**,**b**), which was stored under an argon atmosphere.

2-[2-(2-Methoxyethoxy)ethoxy]ethyl 1-Methylene-3-(4-methylphenyl)-1*H*-indene-2-carboxylate (1a). This monomer was prepared from indenol **3a** (0.60 g, 1.4 mmol). ^{1}H NMR (200 MHz, $CDCl_3$): 2.41 (s, 3H), 3.34 (s, 3H), 3.51 (m, 10H), 4.26 (t, J = 4.9, 2H), 6.36 (s, 1H), 6.60 (s, 1H), 7.23−7.39 (m, 7H), 7.70 (m, 1H). MS(ESI): m/z 431 (M + Na^+).

2,5,8,11,14,17,20,23,26-Nonaoxaoctacosan-28-yl 1-Methylene-3-(4-methylphenyl)-1*H*-indene-2-carboxylate (1b). This monomer was prepared from indenol **3b** (2.6 g, 3.76 mmol). ^{1}H NMR (400 MHz, $CDCl_3$): 2.38 (s, 3H), 3.32 (s, 3H), 3.44 (t, J = 4.7, 2H), 3.48−3.60 (m, 32H), 4.23 (t, J = 4.9, 2H), 6.33 (s, 1H), 6.56 (s, 1H), 7.21−7.31 (m, 7H), 7.67 (d, J = 7.4, 1H). MS(ESI): m/z 695 (M + Na^+).

General Procedure for the Preparation of Poly-Benzofulvene Derivatives Poly-1a,b by Spontaneous Polymerization. The solution of the appropriate benzofulvene macromonomer (**1a**,**b**) in chloroform was concentrated under reduced pressure to give a viscous oil, which was dissolved in chloroform (10 mL/ 1 mmol of monomer) and newly evaporated (this procedure of dissolution/evaporation was repeated four times). The final residue was purified by washing with the appropriate solvents and dried under reduced pressure to obtain the expected polymers (poly-**1a**,**b**).

Poly[2-[2-(2-Methoxyethoxy)ethoxy]ethyl 1-Methylene-3-(4-methylphenyl)-1*H*-indene-2-carboxylate] (Poly-1a). This polymer was prepared from monomer **1a** and purified by washing with petroleum ether to obtain a glassy colorless solid (yield 75%). ^{1}H NMR (200 MHz, $CDCl_3$): 2.2 (br s, 3H), 2.8−3.7 (br m, 17H), 5.3−7.2 (br m, 8H).^{13}C NMR (100 MHz, $CDCl_3$): 21.1, 48.3, 57.6, 59.0, 62.2, 68.2, 70.1, 70.5, 71.9, 122.7, 126.3, 129.5, 131.5, 133.5, 135.7, 142.3, 148.4, 150.8, 163.4. Anal. Calcd for $[(C_{25}H_{28}O_5)_n \cdot (n/2)H_2O]$: C, 71.92; H, 7.00. Found: C, 71.76; H, 6.94.

Poly(2,5,8,11,14,17,20,23,26-Nonaoxaoctacosan-28-yl1-Methylene-3-(4-methylphenyl)-1*H*-indene-2-carboxylate) (Poly-1b). This polymer was obtained from monomer **1b** and purified by washing with diethyl ether to give a colorless gummy solid (yield 92%). ^{1}H NMR (200 MHz, DMSO-d_6): 2.3 (br s, 3H), 2.7−4.0 (br m, 41H), 5.4−7.9 (br m, 8H). Anal. Calcd for $[(C_{37}H_{52}O_{11})_n \cdot nH_2O]$: C, 64.33; H, 7.88. Found: C, 64.20; H, 7.73.

SEC-MALS. The MWD characterization of poly-**BF1** samples was performed by a MALS light scattering photometer online to a SEC chromatographic system. The SEC-MALS system and the corresponding experimental conditions were identical with those used in our previous study[13,14,17] and are not reported in detail here.

Mass Spectrometry. MALDI-TOF mass spectra of poly-**1a**,**b** were recorded in linear mode, using a Voyager-DE STR (Perseptive Biosystem) mass spectrometer, equipped with a nitrogen laser emitting at 337 nm, with a 3 ns pulse width, and working in positive ion mode. The accelerating voltage was 25 KV, the grid voltage and delay time (delayed extraction, time lag) were optimized for each sample to achieve the higher mass resolution, expressed as the molar mass of a given ion divided by the full width at half-maximum (fwhm). The laser irradiance was maintained slightly above the threshold. 2-(4-Hydroxylphenylazo)benzoic acid (HABA) 0.1 M in hexafluoro-2-propanol (HFIP) solvent, was used as matrix. Generally 0.5 mL of a $CHCl_3$ solution of copolymer (5 mg/mL) was mixed with 0.5 mL of a matrix solution, and then spotted on the MALDI sample holder and slowly dried to allow matrix crystallization. The accuracy of mass determination was about 250 ppm in the mass range 1000−2300 Da and 400 ppm in the mass range 2300−5000 Da.

Differential Scanning Calorimetry. Differential scanning calorimetry (DSC) was carried out on a Perkin-Elmer Pyris 1 instrument calibrated with an indium standard. The sample, ca. 5 mg, was placed in a sealed aluminum pan and the measurements were carried out using a heating rate of 20 °C/min over a temperature range of 50−280 °C.

Thermogravimetric Analysis. TGA was performed on a Perkin-Elmer TGA-7 instrument with platinum pan with about 4 mg of material as probe. The sample was heated at 10 °C/min in nitrogen atmosphere under a flow rate of 50 mL/min. TGA and DTG curves were recorded from 50 to 600 °C.

Rheological Measurements. Hydrogel rheological characterization was performed, at 25 °C, by means of a controlled stress rheometer Haake Rheo-Stress RS150, with, as measuring device, a shagreened plate and plate apparatus (PP35 TI: diameter φ = 20 mm; gap between plates = 2 mm). This kind of device was used in order to avoid possible slippage phenomena at the wall. The linear viscoelastic range was determined by means of a stress sweep test consisting in the measuring of elastic (G') and viscous (G'') moduli variation with increasing deformation (γ) being the solicitation frequency f = 1 Hz ($\omega = 2\pi f$ = 6.28 rad/s). The hydrogel mechanical spectrum was determined according to a frequency sweep test consisting in the measurement of elastic (G') and viscous (G'') moduli variation with decreasing pulsation ω at constant deformation γ = 0.01 (well within the linear viscoelastic range).

Low Field NMR Measurements. Hydrogel low field NMR characterization was performed by means of a Bruker Minispec mq20 (0.47 T). Transverse relaxation time (T_2) measurement was made according to CPMG (Carr−Purcell−Meiboom−Gill) sequence with 90−180° pulse separation of 1 ms (number of scans 4; recycle delay 5 s). T_2 distribution was determined by first fitting experimental relaxation data by a sum of exponential functions (S) whose number minimized the product $\chi^2 N_p$, where χ^2 is data fitting chi-square while N_p is the number of model parameters used (each exponential function considered involves 2 parameters: the pre-exponetial factor, A_i, and relaxation time T_{2i}). Then, the continuous relaxation time distribution derives from the iterative solution of a linear system of equation whose unknowns represent the desired distribution and whose right-hand side column vector represents $S(t_j)$ (t_j is the generic instant time). The system matrix coefficient derives from $S(t_j, T_2)$ integration (trapezoid rule) on the continuous relaxation time distribution ($T_{2min} - T_{2max}$).

Cytotoxicity Assays. The human hepatocellular carcinoma lines HepG2 and JHH6 cell lines were cultured in Dulbecco's modified Eagle's medium (DMEM) (Euroclone, Celbio, Devon, U.K.) and in William's medium E (Sigma-Aldrich, St Louis, MO), respectively, at 37 °C and 5% CO_2. All media contained 10% fetal bovine serum (FBS), 2 mM L-glutamine, 100 U/mL penicillin and 100 mg/mL streptomycin (Euroclone, Celbio, Devon, U.K.). Cells were seeded at 3×10^3 cell/well in 200 μL of complete medium in a 96-well microtiter plate and allowed to adhere overnight. The polymer, dissolved by vigorous shaking in sterile water at 42 °C for 30 h, was subsequently added to the cells. After either 1 or 2 days of incubation, an aliquot of the cell culture medium/well was used to evaluate the amount of lactate dehydrogenase (LDH) by the LDH assay kit according to manufacturer's instructions (Bio-Vision Prod., Mountain View CA). As positive control, triton X-100-treated cells (1% of final concentration) were also included in the experimental setup. B3-(4,5-dimethylthiazol-2-yl)-2,5-diphenyltetrazolium bromide (MTT test, Sigma-Aldrich, St Louis, MO) test was then conducted on the cells according to the standard procedures.

Acknowledgment. Thanks are due to Italian MUR (Ministero dell'Università e della Ricerca) for financial support. This work was also partially supported by the "Fondazione Cassa di Risparmio of Trieste", by the "Fondazione Benefica Kathleen Foreman Casali of Trieste" and by "Fondo Trieste 2006. Prof. Stefania D'Agata D'Ottavi's careful reading of the manuscript and Dr Roberto Beretta's and Mr Giulio Zannoni's technical assistance are also acknowledged.

References and Notes

(1) Duncan, R. *Nat. Rev. Drug Discovery* **2003**, *2*, 347–360.
(2) Langer, R. *Science* **1990**, *249*, 1527–1533.
(3) Langer, R. *Nature* **1998**, *392* (suppl), 5–10.
(4) Peracchia, M. T.; Vauthier, C.; Puisieux, F.; Couvreur, P. *J. Biomed. Mat. Res.* **1997**, *34*, 317–326.
(5) Lutz, J.-F.; Andrieu, J.; Uzgiin, S.; Rudolph, C.; Agarwal, S. *Macromolecules* **2007**, *40*, 8540–8543.
(6) Lutz, J.-F.; Hoth, A. *Macromolecules* **2006**, *39*, 893–896.
(7) Oh, J. K.; Min, K.; Matyjaszewski, K. *Macromolecules.* **2006**, *39*, 3161–3167.
(8) Tao, L.; Mantovani, G.; Lecolley, F.; Haddleton, D. M. *J. Am. Chem. Soc.* **2004**, *126*, 13220–13221.
(9) Ishizone, T.; Seki, A.; Hagiwara, M.; Han, S.; Yokoyama, H.; Oyane, A.; Deffieux, A.; Carlotti, S. *Macromolecules* **2008**, *41*, 2963–2967.
(10) Wang, X.-S.; Armes, S. P. *Macromolecules* **2000**, *33*, 6640–6647.
(11) Wang, X.-S.; Lascelles, S. F.; Jackson, R. A.; Armes, S. P. *Chem. Commun.* **1999**, 1817–1818.
(12) Zhang, M.; Müller, A. H. E. *J. Polym. Sci., Part A: Polym. Chem.* **2005**, *43*, 3461–3481.
(13) Cappelli, A.; Pericot Mohr, G.; Anzini, M.; Vomero, S.; Donati, A.; Casolaro, M.; Mendichi, R.; Giorgi, G.; Makovec, F. *J. Org. Chem.* **2003**, *68*, 9473–9476.
(14) Cappelli, A.; Anzini, M.; Vomero, S.; Donati, A.; Zetta, L.; Mendichi, R.; Casolaro, M.; Lupetti, P.; Salvatici, P.; Giorgi, G. *J. Polym. Sci. Part A: Polym. Chem.* **2005**, *43*, 3289–3304.
(15) Cappelli, A.; Galeazzi, S.; Giuliani, G.; Anzini, M.; Aggravi, M.; Donati, A.; Zetta, L.; Boccia, A. C.; Mendichi, R.; Giorgi, G.; Paccagnini, E.; Vomero, S. *Macromolecules* **2008**, *41*, 2324–2334.
(16) Cappelli, A.; Pericot Mohr, G.; Giuliani, G.; Galeazzi, S.; Anzini, M.; Mennuni, L.; Ferrari, F.; Makovec, F.; Kleinrath, E. M.; Langer, T.; Valoti, M.; Giorgi, G.; Vomero, S. *J. Med. Chem.* **2006**, *49*, 6451–6464.
(17) Cappelli, A.; Galeazzi, S.; Giuliani, G.; Anzini, M.; Donati, A.; Zetta, L.; Mendichi, R.; Aggravi, M.; Giorgi, G.; Paccagnini, E.; Vomero, S. *Macromolecules* **2007**, *40*, 3005–3014.
(18) Brockmann, T. W.; Tour, J. *J. Am. Chem. Soc.* **1995**, *117*, 4437–4447.
(19) Londergan, T.; Teng, C. J.; Weber, W. P. *Macromolecules* **1999**, *32*, 1111–1114.
(20) Montaudo, G., Montaudo, M. S., Samperi, F. In *Mass Spectrometry of Polymers*, Montaudo, G., Lattimer, R. P., Eds. CRC Press: Boca Raton, FL, 2002; Chapters 2 and 10.
(21) Montaudo, G.; Montaudo, M. S.; Samperi, F. *Prog. Polym. Sci.* **2006**, *31*, 277–357.
(22) Vauthier, C.; Dubernet, C.; Fattal, E.; Pinto-Alphandary, H.; Couvreur, P. *Adv. Drug Delivery Rev.* **2003**, *55*, 519–548.
(23) Pepper, D. C. *J. Polym. Sci. Polym. Symp.* **1978**, *62*, 65–77.
(24) Lapasin, R.; Pricl, S. *Rheology of Industrial Polysaccharides, Theory and Applications*; Chapman & Hall: London, 1995.
(25) Pasut, E.; Toffanin, R.; Voinovich, D.; Pedersini, C.; Murano, E.; Grassi, M. *J. Biomed. Mater. Res. A*, **2008**, *87*, 808−818.
(26) Flory, P. J. *Principles of Polymer Chemistry*, Cornell University: Ithaca, NY, 1953.
(27) Schurz, J. *Prog. Polym. Sci.* **1991**, *16*, 1–53.
(28) Halperin, W. P.; D'Orazio, F.; Bhattacharja, S.; Tarczon T. C. *Magnetic Resonance Relaxation Analysis of Porous Media*; John Wiley and Sons: New York, 1989.
(29) Brownstein, K. R.; Tarr, C. E. *Phys. Rev. A* **1979**, *19*, 2446–2452.
(30) Coviello, T.; Coluzzi, G.; Palleschi, A.; Grassi, M.; Santucci, E.; Alhaique, F. *Int. J. Biol. Macromol.* **2003**, *32*, 83–92.
(31) Lustig, S. R.; Peppas, N. A. *J. Appl. Polym. Sci.* **1988**, *36*, 735–747.
(32) Grassi, G.; Scaggiante, B.; Farra, R.; Dapas, B.; Agostini, F.; Baiz, D.; Rosso, N.; Tiribelli, C. *Biochimie* **2007**, *89*, 1544–1552.
(33) Shapland, P. D. P. Process for Preparing Nonaethylene Glycol Monomethyl Ether. WO 2005/102976.

MA802429G